Bioorganic Chemistry 89 (2019) 102943

Contents lists available at ScienceDirect

Bioorganic Chemistry

journal homepage: www.elsevier.com/locate/bioorg

Discovery of pyrazolopyrimidine derivatives as potent BTK inhibitors with effective anticancer activity in MCL

Fansheng Ran[a], Yang Liu[b], Meixia Liu[a], Daoguang Zhang[a], Peng Wang[c], Junze Dong[a], Wendi Tang[a], Guisen Zhao[a,*]

[a] Department of Medicinal Chemistry, Key Laboratory of Chemical Biology (Ministry of Education), School of Pharmaceutical Sciences, Shandong University, 44 West Culture Road, Jinan 250012, PR China
[b] Department of Lymphoma and Myeloma, The University of Texas MD Anderson Cancer Center, Houston, TX 77030, USA
[c] Shandong Qidu Pharmaceutical Co., Ltd., 28 Renmin East Road, Zibo 255400, PR China

ARTICLE INFO

Keywords:
Mantle cell lymphoma
BTK inhibitors
Anticancer
Selectivity
Patient cells

ABSTRACT

Bruton's tyrosine kinase (BTK) is a key regulator of B-cell receptor (BCR) signaling pathway and takes effect in the regulation of B-cell activation, survival, proliferation and differentiation. It has been proved that BTK is commonly overexpressed in mantle cell lymphoma (MCL), which makes it a focus of targeted therapy for MCL. Our studies yielded a novel series of pyrazolopyrimidine derivatives capable of potent inhibition of BTK. Notably, **12a** showed higher selectivity against BTK and exhibited robust antiproliferative effects in both mantle cell lymphoma cell lines and primary patient tumor cells. Low micromolar doses of **12a** induced strong cell apoptosis in Jeko-1 and Z138 cells.

1. Introduction

Mantle cell lymphoma (MCL) is an aggressive, largely incurable B cell Non-Hodgkin's Lymphoma (NHL) with poor prognosis and over-expression of the cell cycle protein, cyclin-D1 [1–4]. Activation of cell survival pathways is involved in the development of MCL [5]. Bruton's tyrosine kinase (BTK), which is a non-receptor cytoplasmic protein tyrosine kinase belonging to the Tec kinase family, expresses in immune cells like B cells, mast cells and macrophages [6–9]. BTK is a key regulator of BCR signaling pathway and plays an important role in the regulation of B-cell activation, survival, proliferation and differentiation [10–12]. Upon BCR activation, BTK is transported to the membrane and initially phosphorylated at Y551 by Syk and Lyn, followed by autophosphorylation at Y223 and becomes physiologically active [13]. In turn, it induces the activation of PLCγ and other signaling pathways such as PI3K/Akt/mTOR and NF-κB [6,14]. Deregulation of BTK has been observed in MCL, chronic lymphocytic leukemia (CLL), acute myeloid leukemia (AML) and activated B-cell-diffuse large B-cell lymphoma [15–19]. Thus, BTK is considered as a prospective target for the treatment of autoimmune diseases and cancer.

During recent years, many small-molecule inhibitors of BTK have been reported, which can be classified into two classes by their binding modes with the BTK catalytic domains, irreversible inhibitors and reversible inhibitors [20]. Irreversible BTK inhibitors keep warheads such as the acrylamide group and chloroacetamide group in the structures which can form a covalent bond by Michael addition, nucleophilic addition, addition-elimination or nucleophilic substitution reactions with the conserved noncatalytic cysteine residue (Cys481) of BTK to achieve strong binding [21]. Ibrutinib (**IBN**, **1**), a first-in-class irreversible BTK inhibitor, has been approved by FDA to treat MCL, CLL and Waldenström's macroglobulinemia (WM) [16,22–24]. Recently, acalabrutinib (**ACP-196**, **2**) was also approved by FDA to treat MCL [25–26]. Moreover, a number of covalent and noncovalent BTK inhibitors including **GS-4059** (**3**) [27], **CC-292** (**4**) [28], **HM71224** (**5**) [29], **PLS-123** (**6**) [30] and **7** [31] have been advanced to preclinical or clinical trials to treat autoimmune diseases (Fig. 1).

All the above inhibitors share a common feature (Fig. 2A): an aromatic core structure to occupy the hinge region of BTK; a large hydrophobic group extending to the hydrophobic pockets beside the hinge region; on the other side, the linker connected the warheads in irreversible BTK inhibitors extending to Cys481 of BTK forming a covalent bind, or linkers attached to the terminal groups in reversible BTK inhibitors spreading to the solvent region (Fig. 2A) [26,32–34]. Among the reported BTK inhibitors, the piperidine ring, phenyl ring and pyrrole ring were the common linkers (Fig. 1). In our design, the backbone and hydrophobic groups of **IBN** were retained and the piperidine linker

* Corresponding author.
E-mail address: guisenzhao@sdu.edu.cn (G. Zhao).

https://doi.org/10.1016/j.bioorg.2019.102943
Received 9 December 2018; Received in revised form 3 April 2019; Accepted 19 April 2019
Available online 25 April 2019

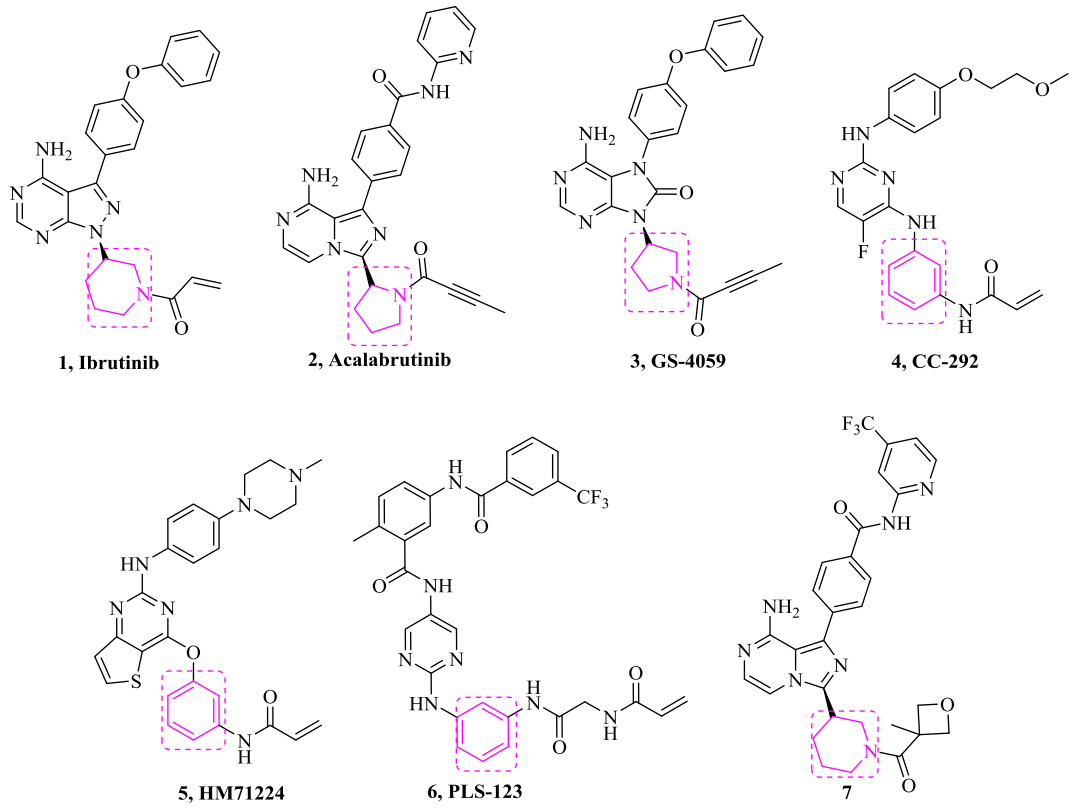

Fig. 1. Representative chemical structures of the novel BTK inhibitors.

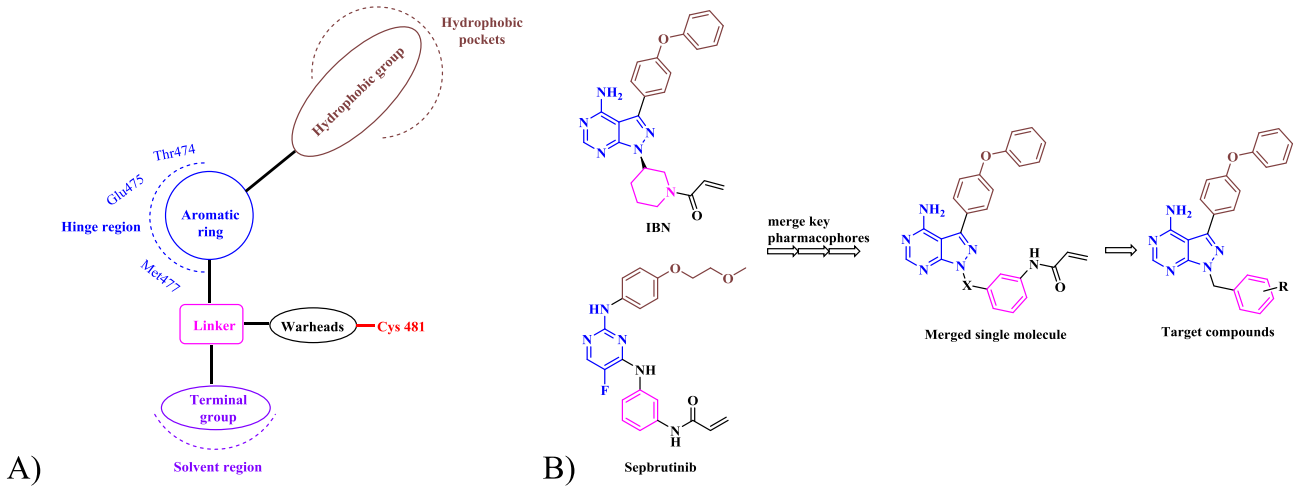

Fig. 2. (A) Common features of BTK inhibitors; (B) Design of target compounds.

was replaced by the phenyl ring which was attached to the nucleus via a methylene group. A series of pyrrolopyrimidine derivatives as novel potent BTK inhibitors was reported herein (Fig. 2B).

2. Results and discussion

2.1. Chemistry

The synthetic routes for these compounds are illustrated in Scheme 1. *N*-alkylation of compound **8** [35] with appropriately substituted benzyl bromides (**9**) gave us the target compounds **10**. Reduction of the nitro groups on compounds **10a** and **10b** under the presence of Fe-NH_4Cl yielded compounds **11a** and **11b**, respectively. Following condensation of compound **11a** and different acyl chlorides afforded the final products **12**.

2.2. BTK inhibitory activity

The newly synthesized pyrazolopyrimidine analogs were evaluated for their activity against BTK via a KinaseProfiler radiometric protein kinase assay. First, we performed the initial screening at 1 μM concentration. Next, we selected compounds with BTK inhibition rate > 80% at 1 μM to test the IC_{50} values. The results were shown in Table 1. Compound **10c** with a hydrogen atom at the R group showed moderate BTK inhibitory activity (**10c** IC_{50} = 229 nM). Introduction of the methyl group (R) at the aromatic ring represented an obvious

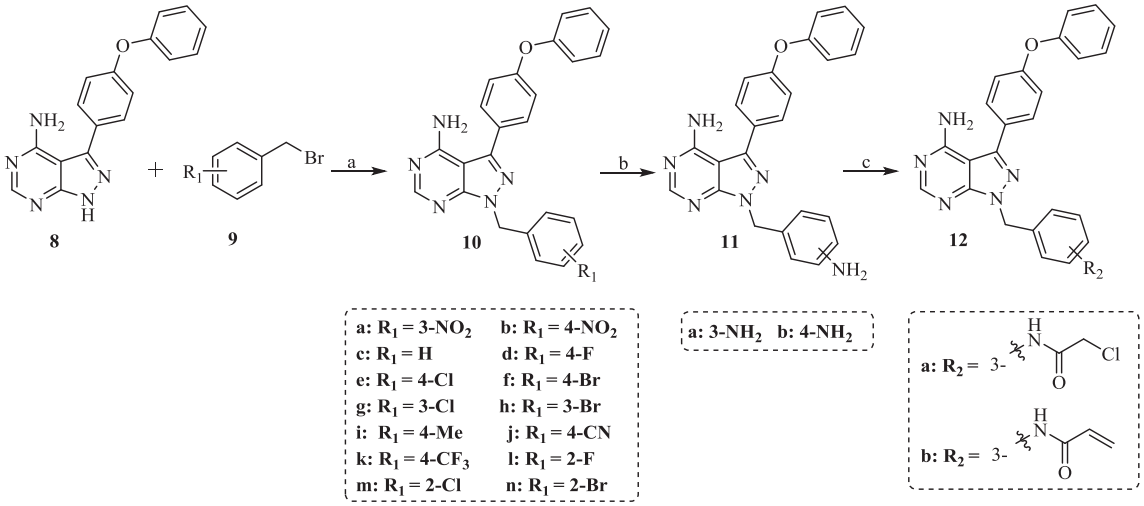

Scheme 1. Synthetic route of the compounds **10**, **11** and **12**. Reagents and conditions: (a) K_2CO_3, DMF, r.t., 5 h; (b) Fe, NH_4Cl, ethanol/water = 3/1, reflux, 6 h; (c) acyl chloride, Et_3N, THF, 0 °C to r.t., 5 h.

improvement in BTK inhibition over the introduction of the cyanide and trifluoromethyl groups (**10i** *vs* **10j** or **10 k**). The amino group was more beneficial to BTK inhibitory activity than the nitro group (**11b** *vs* **10b**). Amino substituent on the meta-position and para-position produced an equivalent profile (**11a** *vs* **11b**). Compared with the chlorine and bromine substitution, the fluorine substituent displayed the best efficacy against BTK (**10 l** IC_{50} = 39 nM, **10 m** IC_{50} = 129 nM and **10n** IC_{50} = 88 nM). Introducing the warheads, the chloroacetamide group or acrylamide group, significantly increased the BTK inhibitory activity (**12a** *vs* **11a** and **12b** *vs* **11a**). Among these compounds, **12a** exhibited the strongest BTK inhibitory activity, slightly weaker than **IBN** (**12a** IC_{50} = 27 nM, **IBN** IC_{50} = 8 nM).

2.3. Cell viability assay in MCL cell lines

According to the CellTiter-Glo Luminescent cell viability assay protocol, several compounds that had potent inhibitory activity against BTK were determined for their antiproliferative activity in MCL cells. The tested cell lines included Mino, Jeko-1, Z138, Maver-1 and BTK knock out Jeko-1 cells. As shown in Table 2, amino substituent on the meta-position was more useful for antiproliferative activity than the para-position (**11a** *vs* **11b**). Compared with **IBN**, both compounds **12a** and **12b** demonstrated improved antiproliferative activities in MCL cell lines. **12a** was the most potent anticancer agent in MCL cells with IC_{50} values lower than 1 μM.

Table 2
Cell proliferation assay assessing the effects of compounds on MCL cell lines.

Compd	Cell viability assay, IC_{50} μM				
	Mino	Jeko-1	Z138	Maver-1	BTK knock out Jeko-1
IBN	15.7	1.1	9.7	7.8	8.7
10l	11.1	32.9	43.7	34.3	ND[a]
11a	9.5	11.2	14.2	16.8	16.7
11b	13.9	13.2	18.4	18.7	17.9
12a	0.9	0.4	0.8	0.4	0.8
12b	1.3	1.3	2.8	2.6	3.5

[a] ND: not detected.

2.4. Cell apoptosis assay

We proceeded to test the effects of **12a** on apoptosis in Jeko-1 and Z138 cells via an annexin V-FITC/propidium iodide (PI) binding assay. As shown in Fig. 3, after 24 h of treatment, a deep degree of apoptosis was observed in Jeko-1 and Z138 cells. Compound **12a** triggered dose-

Table 1
The inhibitory effects of series **10**, **11** and **12** on BTK activity.

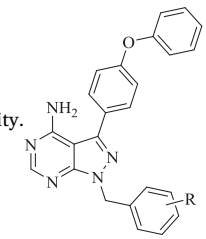

Compd	R	BTK inhibition (%) at 1 μM	BTK IC_{50} (nM)	Compd	R	BTK inhibition (%) at 1 μM	BTK IC_{50} (nM)
IBN	–	100	8	**10j**	4-CN	12	ND[a]
10b	4-NO_2	67	ND[a]	**10k**	4-CF_3	27	ND[a]
10c	H	81	229	**10l**	2-F	92	39
10d	4-F	79	ND[a]	**10m**	2-Cl	91	129
10e	4-Cl	44	ND[a]	**10n**	2-Br	93	88
10f	4-Br	28	ND[a]	**11a**	3-NH_2	90	75
10g	3-Cl	60	ND[a]	**11b**	4-NH_2	93	82
10h	3-Br	49	ND[a]	**12a**	3-$NHCOCH_2Cl$	98	27
10i	4-Me	66	ND[a]	**12b**	3-NHCOCH = CH_2	97	50

[a] ND: not detected.

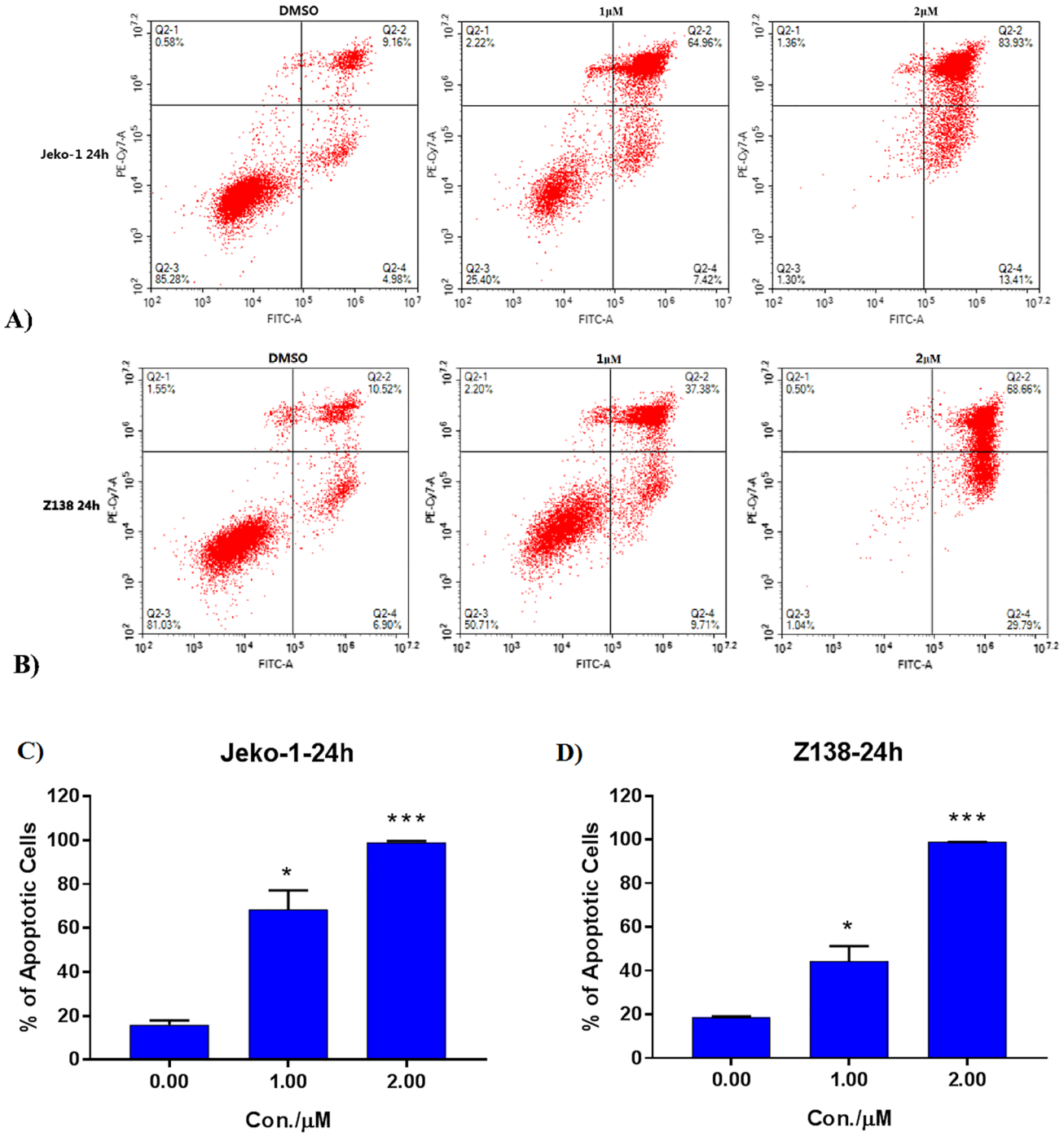

Fig. 3. Cell apoptosis assay for **12a** in Jeko-1 and Z138 cells. (A/C) Apoptosis assay of **12a** at indicated concentrations in Jeko-1 cells for 24 h; (B/D) Apoptosis assay of **12a** at indicated concentrations in Z138 cells for 24 h. The data shown are the mean of three independent experiments. Statistical significance is indicated as *P < 0.05, **P < 0.01, ***P < 0.001 compared with the DMSO control.

dependent apoptosis of the cells with ratios of 72% and 97% at concentrations of 1 μM and 2 μM compared with 14% in control in Jeko-1 cells; high percentage of apoptosis was also observed in Z138 cells after **12a** treatment.

2.5. Cell viability assay in primary MCL cells

We investigated the antiproliferative efficacy of compounds **12a** and **IBN** in primary MCL patient cells. As shown in Fig. 4, **12a** demonstrated more potent antiproliferative activity in these cells than **IBN**. This result is consistent with that in MCL cells.

2.6. Selectivity over other kinases

Compound **12a** was selected for further investigation because of its good BTK enzymatic potency, potent anti-proliferative activity and strong apoptosis inductive effect in MCL cell lines. We further tested the biochemical activity of compound **12a** against a panel of 12 kinases at the concentration of 1 μM. The results of kinases screening were listed in Table 3. Compound **12a** lacked selectivity for Tec kinase family members including Tec, Bmx and Txk, which is the same as **IBN**. Moderate inhibitory activity against Csk (53%), JAK3 (47%) and SRM (70%) was observed. Compared to **IBN**, compound **12a** expressed no

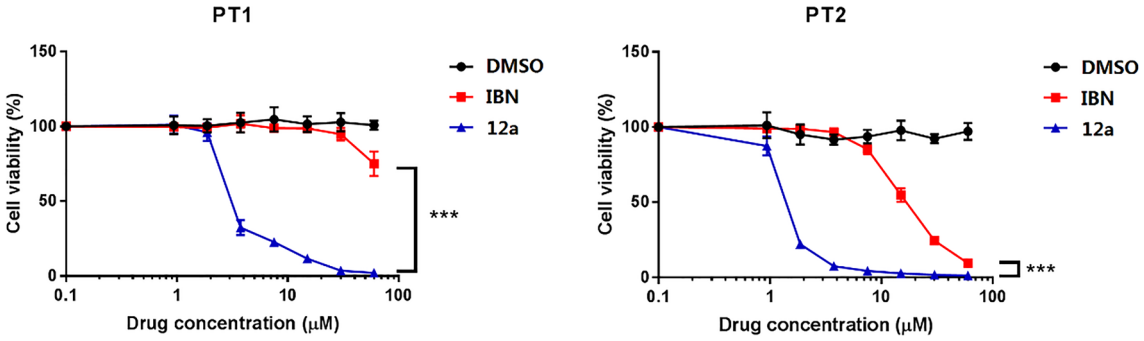

Fig. 4. Cell viability assay after 24 h treatment of **12a** and **IBN** in two naïve MCL patient cells.

Table 3
Inhibition efficacy (%) among different kinases at 1 μM by **12a** and **IBN**.

Kinases	**12a**	IBN	Kinases	**12a**	IBN
Tec	92	103	ErbB2	31	73
Bmx	99	102	B-raf	−2	19
Txk	87	97	Flt3	1	8
Itk	26	86	JAK3	47	54
Csk	53	87	PTK5	31	91
EGFR	15	98	SRM	70	100

inhibition activity against Itk, EGFR, B-raf, Flt3, PTK5 and ErbB2 (inhibitory activities at 1 μM < 40% [36]), indicating greater BTK selectivity than **IBN** and potential safety improvement for the treatment of MCL.

2.7. Molecular modeling

The result of compound **12a** with BTK on molecular modeling was shown in Fig. 5. The pyrazolopyrimidine core formed several important hydrogen bonds with the hinge region through Glu475 and Met477 and the diphenyl ether group extended to the hydrophobic pocket behind the gatekeeper Thr474 displaying an edge-to-face aromatic interaction with Phe540. The acylamide group formed a hydrogen bond with the backbone carbonyl of Arg525. The chloroacetyl group of **12a** was about 5.8 Å away from the sulfhydryl group of BTK Cys481 and could form the covalent bond with Cys481 by nucleophilic substitution.

3. Conclusion

In summary, this study outlined the design, synthesis and biological evaluation of novel pyrazolopyrimidine derivatives as potential agents for treating MCL. Among these compounds, **12a** exhibited potent BTK inhibitory activity and high selectivity. Compound **12a** exhibited robust antiproliferative effects in primary patient tumor cells and showed strong apoptosis induction in Jeko-1 and Z138 cells. Compared with **IBN**, **12a** improved antiproliferative activities 2–19 folds in MCL cell lines with IC_{50} values lower than 1 μM, supporting further evaluation and development of the promising candidate **12a** in cancer therapy.

4. Experimental section

4.1. Chemistry

All the chemical reagents and solvents were purchased from commercial sources and used without further purification. Reactions were monitored using thin-layer chromatography (TLC) performed on SGF254 plates. Column chromatography was carried out with the indicated solvents using silica gel (60 Å, 200–300 mesh). Melting points were determined using Büchi capillary melting point apparatus (Buchi Labortechnik AG, Switzerland) without correction. Using tetramethylsilane (TMS) as an internal standard in DMSO-d_6 or $CDCl_3$, NMR spectra was recorded at 400 MHz for ^1H and 100 MHz for ^{13}C on a Bruker Avance DRX-400 Spectrometer (Bruker, Germany). The chemical shifts (δ) were reported in parts per million (ppm) using tetramethylsilane as internal standard.

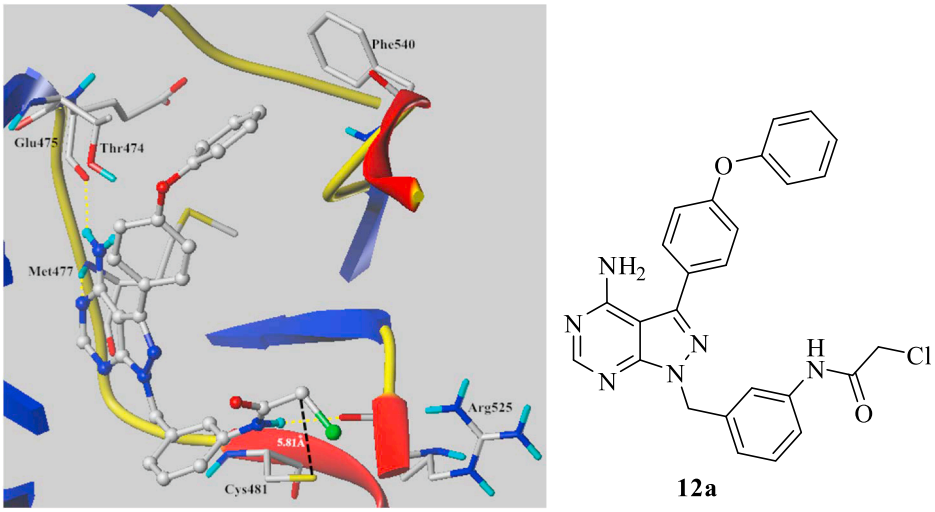

Fig. 5. Molecular docking mode of **12a** with BTK. PDB ID: 3gen.

4.2. General synthesis of compounds

4.2.1. General procedure for the synthesis of **10a–10n**

To a solution of **8** (1 mmol) and substituted benzyl bromide **9** (1.2 mmol) in *N*, *N*-dimethylformamide (5 mL) was added K_2CO_3 (1.5 mmol) and the reaction mixture was stirred for 5 h at room temperature. The reaction solution was poured into water (50 mL). The suspension was filtered and the crude product was purified by silica gel column chromatography with dichloromethane/methanol (80/1–40/1) to give target compounds **10a** − **10n**.

*4.2.1.1. 1-(3-nitrobenzyl)-3-(4-phenoxyphenyl)-1H-pyrazolo[3,4-d] pyrimidin-4-amine (**10a**)*. Pale yellow solid, yield 63%, Mp: 169–171 °C, ^{1}H NMR (400 MHz, DMSO-d_6) δ 8.31 (s, 1H), 8.17 (d, J = 12.0 Hz, 2H), 7.78–7.61 (m, 5H), 7.44 (t, J = 7.9 Hz, 2H), 7.25–7.05 (m, 6H), 5.73 (s, 2H). ^{13}C NMR (100 MHz, DMSO-d_6) δ 158.74, 157.69, 156.69, 156.67, 155.01, 148.29, 144.57, 139.81, 134.75, 130.76, 130.60, 130.54, 128.07, 124.29, 123.11, 122.74, 119.48, 119.43, 97.79, 49.36. ESI-MS: m/z 439.28 (M + H$^+$).

*4.2.1.2. 1-(4-Nitrobenzyl)-3-(4-phenoxyphenyl)-1H-pyrazolo[3,4-d] pyrimidin-4-amine (**10b**)*. Pale yellow solid, yield 75%, Mp: 178–181 °C, ^{1}H NMR (400 MHz, DMSO-d_6) δ 8.31 (s, 1H), 8.20 (d, J = 8.4 Hz, 3H), 7.69 (d, J = 8.3 Hz, 2H), 7.56–7.40 (m, 5H), 7.23–7.09 (m, 5H), 5.73 (s, 2H). ^{13}C NMR (100 MHz, DMSO-d_6) δ 158.75, 157.70, 156.71, 156.66, 155.09, 147.38, 145.21, 144.62, 130.60, 130.55, 129.18, 129.13, 128.09, 124.29, 119.48, 119.43, 97.80, 49.57. ESI-MS: m/z 439.21 (M + H$^+$).

*4.2.1.3. 1-Benzyl-3-(4-phenoxyphenyl)-1H-pyrazolo[3,4-d] pyrimidin-4-amine (**10c**)*. White solid, yield 77%, Mp: 158–160 °C, ^{1}H NMR (400 MHz, DMSO-d_6) δ 8.29 (s, 1H), 7.66 (d, J = 8.5 Hz, 2H), 7.43 (t, J = 7.9 Hz, 2H), 7.36–7.25 (m, 6H), 7.22–7.06 (m, 6H), 5.56 (s, 2H). ^{13}C NMR (100 MHz, DMSO-d_6) δ 158.70, 157.60, 156.77, 156.49, 154.85, 144.06, 137.67, 130.60, 130.52, 129.04, 128.30, 128.10, 128.04, 124.27, 119.40, 97.75, 50.26. ESI-MS: m/z 394.17 (M + H$^+$).

*4.2.1.4. 1-(4-Fluorobenzyl)-3-(4-phenoxyphenyl)-1H-pyrazolo[3,4-d] pyrimidin-4-amine (**10d**)*. White solid, yield 68%, Mp: 182–185 °C, ^{1}H NMR (400 MHz, DMSO-d_6) δ 8.29 (s, 1H), 7.66 (d, J = 8.5 Hz, 2H), 7.44 (t, J = 7.9 Hz, 2H), 7.36 (dd, J = 8.3, 5.7 Hz, 2H), 7.21–7.11 (m, 9H), 5.55 (s, 2H). ^{13}C NMR (100 MHz, DMSO-d_6) δ 163.25, 160.83, 158.70, 157.62, 156.75, 156.52, 154.78, 144.16, 133.89, 133.86, 130.60, 130.53, 130.31, 130.23, 128.24, 124.27, 119.46, 115.96, 115.75, 97.76, 49.51. ESI-MS: m/z 412.29 (M + H$^+$).

*4.2.1.5. 1-(4-Chlorobenzyl)-3-(4-phenoxyphenyl)-1H-pyrazolo[3,4-d] pyrimidin-4-amine (**10e**)*. White solid, yield 81%, Mp: 200–202 °C, ^{1}H NMR (400 MHz, DMSO-d_6) δ 8.29 (s, 1H), 7.66 (d, J = 8.6 Hz, 2H), 7.47–7.38 (m, 5H), 7.31 (d, J = 8.4 Hz, 2H), 7.21–7.11 (m, 6H), 5.56 (s, 2H). ^{13}C NMR (100 MHz, DMSO-d_6) δ 158.70, 157.64, 156.74, 156.54, 154.86, 144.25, 136.65, 132.72, 130.60, 130.53, 130.01, 129.05, 128.21, 124.28, 119.46, 119.44, 97.76, 49.53. ESI-MS: m/z 428.23 (M + H$^+$).

*4.2.1.6. 1-(4-Bromobenzyl)-3-(4-phenoxyphenyl)-1H-pyrazolo[3,4-d] pyrimidin-4-amine (**10f**)*. White solid, yield 69%, Mp: 207–210 °C, ^{1}H NMR (400 MHz, DMSO-d_6) δ 8.29 (s, 1H), 7.66 (d, J = 8.6 Hz, 2H), 7.53 (d, J = 8.3 Hz, 2H), 7.43 (t, J = 7.9 Hz, 2H), 7.25 (d, J = 8.3 Hz, 2H), 7.20–6.76 (m, 7H), 5.54 (s, 2H). ^{13}C NMR (100 MHz, DMSO-d_6) δ 158.71, 157.64, 156.75, 156.54, 154.88, 144.26, 137.06, 131.98, 130.60, 130.53, 130.34, 128.21, 124.28, 121.25, 119.47, 119.44, 97.77, 49.60. ESI-MS: m/z 472.01 (M + H$^+$).

*4.2.1.7. 1-(3-Chlorobenzyl)-3-(4-phenoxyphenyl)-1H-pyrazolo[3,4-d] pyrimidin-4-amine (**10g**)*. White solid, yield 66%, Mp: 162–164 °C ^{1}H NMR (400 MHz, DMSO-d_6) δ 8.30 (s, 1H), 7.66 (d, J = 7.2 Hz, 2H), 7.45–7.36 (m, 5H), 7.23–7.11 (m, 8H), 5.57 (s, 2H). ^{13}C NMR (100 MHz, DMSO-d_6) δ 158.73, 157.67, 156.73, 156.59, 154.92, 144.35, 140.10, 133.59, 131.03, 130.60, 130.54, 128.17, 128.07, 127.91, 126.77, 124.28, 119.48, 119.44, 97.78, 49.58. ESI-MS: m/z 428.19 (M + H$^+$).

*4.2.1.8. 1-(3-Bromobenzyl)-3-(4-phenoxyphenyl)-1H-pyrazolo[3,4-d] pyrimidin-4-amine (**10h**)*. White solid, yield 77%, Mp: 164–166 °C ^{1}H NMR (400 MHz, DMSO-d_6) δ 8.30 (s, 1H), 7.66 (d, J = 8.4 Hz, 2H), 7.54–7.26 (m, 5H), 7.32–7.26 (m, 2H), 7.22–7.02 (m, 6H), 5.57 (s, 2H). ^{13}C NMR (100 MHz, DMSO-d_6) δ 158.72, 157.67, 156.73, 156.60, 154.91, 144.35, 140.35, 131.33, 130.98, 130.81, 130.60, 130.54, 128.16, 127.17, 124.28, 122.17, 119.48, 119.45, 97.77, 49.52. ESI-MS: m/z 472.17 (M + H$^+$).

*4.2.1.9. 1-(4-Methylbenzyl)-3-(4-phenoxyphenyl)-1H-pyrazolo[3,4-d] pyrimidin-4-amine (**10i**)*. White solid, yield 79%, Mp: 176–179 °C ^{1}H NMR (400 MHz, DMSO-d_6) δ 8.29 (s, 1H), 7.65 (d, J = 8.5 Hz, 2H), 7.43 (t, J = 7.9 Hz, 2H), 7.21–7.10 (m, 11*H*), 5.50 (s, 2H), 2.25 (s, 3H). ^{13}C NMR (100 MHz, DMSO-d_6) δ 158.67, 157.58, 156.78, 156.44, 154.76, 143.95, 137.25, 134.67, 130.60, 130.51, 129.56, 128.34, 128.15, 124.26, 119.45, 97.74, 50.06, 21.14. ESI-MS: m/z 408.18 (M + H$^+$).

*4.2.1.10. 4-((4-Amino-3-(4-phenoxyphenyl)-1H-pyrazolo[3,4-d] pyrimidin-1-yl) methyl) benzonitrile (**10j**)*. White solid, yield 61%, Mp: 178–181 °C ^{1}H NMR (400 MHz, DMSO-d_6) δ 8.29 (s, 1H), 7.81 (d, J = 8.1 Hz, 2H), 7.67 (d, J = 8.5 Hz, 2H), 7.46–7.42 (m, 5H), 7.21–7.11 (m, 6H), 5.67 (s, 2H). ^{13}C NMR (100 MHz, DMSO-d_6) δ 158.75, 157.69, 156.72, 156.65, 155.06, 144.54, 143.27, 133.09, 130.63, 130.57, 128.84, 128.12, 124.31, 119.49, 119.45, 119.16, 110.87, 97.78, 49.79. ESI-MS: m/z 419.24 (M + H$^+$).

*4.2.1.11. 3-(4-Phenoxyphenyl)-1-(4-(trifluoromethyl)benzyl)-1H-pyrazolo [3,4-d]pyrimidin-4-amine (**10k**)*. White solid, yield 78%, Mp: 182–185 °C, ^{1}H NMR (400 MHz, DMSO-d_6) δ 8.29 (s, 1H), 7.69 (dd, J = 15.7, 8.1 Hz, 5H), 7.52–7.38 (m, 4H), 7.23–7.08 (m, 6H), 5.67 (s, 2H). ^{13}C NMR (100 MHz, DMSO-d_6) δ 158.74, 157.68, 156.74, 156.62, 155.03, 144.44, 142.35, 130.61, 130.55, 128.82, 128.77, 128.50, 128.16, 126.07, 126.03, 126.00, 125.96, 124.29, 123.29, 119.48, 119.44, 97.78, 49.73. ESI-MS: m/z 462.31 (M + H$^+$).

*4.2.1.12. 1-(2-Fluorobenzyl)-3-(4-phenoxyphenyl)-1H-pyrazolo[3,4-d] pyrimidin-4-amine (**10l**)*. White solid, yield 80%, Mp: 144–146 °C, ^{1}H NMR (400 MHz, DMSO-d_6) δ 8.29 (s, 1H), 7.65 (d, J = 8.6 Hz, 2H), 7.43 (t, J = 7.9 Hz, 2H), 7.36 (q, J = 6.9 Hz, 1H), 7.25–7.11 (m, 10*H*), 5.61 (s, 2H). ^{13}C NMR (100 MHz, DMSO-d_6) δ 161.55, 159.11, 158.70, 157.63, 156.76, 156.51, 154.98, 144.29, 130.66, 130.62, 130.59, 130.54, 130.41, 130.33, 128.22, 125.11, 125.07, 124.42, 124.26, 119.47, 119.44, 116.01, 115.80, 97.72, 43.95, 43.91. ESI-MS: m/z 412.21 (M + H$^+$).

*4.2.1.13. 1-(2-Chlorobenzyl)-3-(4-phenoxyphenyl)-1H-pyrazolo[3,4-d] pyrimidin-4-amine (**10m**)*. White solid, yield 74%, Mp: 148–151 °C, ^{1}H NMR (400 MHz, DMSO-d_6) δ 8.29 (s, 1H), 7.67 (d, J = 8.5 Hz, 2H), 7.49 (d, J = 7.8 Hz, 1H), 7.42 (t, J = 7.9 Hz, 2H), 7.34–7.25 (m, 2H), 7.21–7.09 (m, 6H), 6.99 (d, J = 7.5 Hz, 1H), 5.65 (s, 2H). ^{13}C NMR (100 MHz, DMSO-d_6) δ 158.74, 157.66, 156.75, 156.55, 155.22, 144.47, 134.89, 132.38, 130.58, 130.55, 129.87, 129.83, 128.20, 127.93, 124.25, 119.46, 119.44, 97.75, 47.77. ESI-MS: m/z 428.21 (M + H$^+$).

*4.2.1.14. 1-(2-Bromobenzyl)-3-(4-phenoxyphenyl)-1H-pyrazolo[3,4-d] pyrimidin-4-amine (**10n**)*. White solid, yield 82%, Mp: 154–157 °C, ^{1}H NMR (400 MHz, DMSO-d_6) δ 8.28 (s, 1H), 7.67 (d, J = 8.3 Hz, 3H), 7.43 (t, J = 7.7 Hz, 2H), 7.32–7.10 (m, 9H), 6.91 (d, J = 7.3 Hz, 1H), 5.62

(s, 2H). ^{13}C NMR (100 MHz, DMSO-d_6) δ 158.75, 157.66, 156.75, 156.57, 155.25, 144.51, 136.49, 133.14, 130.60, 130.56, 130.11, 129.69, 128.50, 128.19, 124.27, 122.45, 119.47, 119.45, 97.75, 50.19. ESI-MS: *m/z* 472.10 ($M+H^+$).

4.2.2. General procedure for the synthesis of **11a** and **11b**

To a mixture of **10a** or **10b** (1 mmol) in the mixed solution of ethanol/water = 3/1 (20 mL) was added Fe (3 mmol) and NH_4Cl (3 mmol). Then the mixture was heated to reflux for 6 h. The reaction mixture was hot filtered and the filtrate was concentrated under reduced pressure. The crude product was purified by silica gel column chromatography with dichloromethane/methanol (110/1–40/1) to yield compounds **11a** or **11b**.

*4.2.2.1. 1-(3-Aminobenzyl)-3-(6-phenoxypyridin-3-yl)-1H-pyrazolo[3,4-d] pyrimidin-4-amine (**11a**)*. White solid, yield 89%, Mp: 160–162 °C, ^{1}H NMR (400 MHz, DMSO-d_6) δ 8.28 (s, 1H), 7.66 (d, J = 8.7 Hz, 2H), 7.43 (t, J = 8.0 Hz, 2H), 7.18–7.11 (m, 6H), 6.94 (t, J = 8.0 Hz, 1H), 6.49–6.41 (m, 4H), 5.37 (s, 2H), 5.11 (s, 2H). ^{13}C NMR (100 MHz, DMSO-d_6) δ 158.66, 157.55, 156.79, 156.38, 154.75, 149.31, 143.79, 138.20, 130.61, 130.53, 129.46, 128.40, 124.26, 119.46, 119.44, 115.48, 113.57, 113.24, 97.69, 50.51. ESI-MS: *m/z* 409.11 ($M+H^+$).

*4.2.2.2. 1-(4-Aminobenzyl)-3-(4-phenoxyphenyl)-1H-pyrazolo[3,4-d] pyrimidin-4-amine (**11b**)*. White solid, yield 86%, Mp:165–168 °C, ^{1}H NMR (400 MHz, DMSO-d_6) δ 8.29 (s, 1H), 7.65 (d, J = 8.5 Hz, 2H), 7.43 (t, J = 7.9 Hz, 2H), 7.21–7.08 (m, 6H), 7.04 (d, J = 8.3 Hz, 2H), 6.50 (d, J = 8.3 Hz, 2H), 5.34 (s, 2H), 5.21 (s, 2H). ^{13}C NMR (100 MHz, DMSO-d_6) δ 158.59, 157.51, 156.79, 156.26, 154.42, 148.51, 143.60, 130.60, 130.50, 129.41, 128.45, 124.62, 124.24, 119.46, 119.43, 114.25, 97.73, 50.20. ESI-MS: *m/z* 408.86 ($M+H^+$).

4.2.3. General procedure for the synthesis of **12a** and **12b**

To a solution of compound **11a** (1 mmol) and triethylamine (3 mmol) in tetrahydrofuran (10 mL), acyl chloride (1.2 mmol) was added under ice-cold conditions. The mixture was stirred at room temperature for 5 h. Upon completion, the reaction mixture was extracted with water and ethyl acetate. The organic layer was dried over Na_2SO_4 and the solvent was evaporated in vacuo. The residue was purified by silica gel column chromatography with dichloromethane/methanol (80/1–40/1) to give target compounds **12a** − **12b**.

*4.2.3.1. N-(3-((4-amino-3-(4-phenoxyphenyl)-1H-pyrazolo[3,4-d] pyrimidin-1-yl)methyl)phenyl)-2-chloroacetamide (**12a**)*. White solid, yield 55%, Mp: 166–168 °C, ^{1}H NMR (400 MHz, DMSO-d_6) δ 10.30 (s, 1H), 8.29 (s, 1H), 7.67 (d, J = 8.6 Hz, 2H), 7.56 (d, J = 8.8 Hz, 1H), 7.46–7.41 (m, 4H), 7.29 (t, J = 7.9 Hz, 1H), 7.20–7.11 (m, 6H), 7.05 (d, J = 7.7 Hz, 1H), 5.53 (s, 2H), 4.20 (s, 2H). ^{13}C NMR (100 MHz, $CDCl_3$) δ 163.76, 158.80, 156.87, 156.21, 154.19, 144.81, 137.36, 137.01, 130.01, 129.96, 129.63, 127.16, 124.90, 124.16, 119.77, 119.62, 119.14, 98.26, 50.70, 42.85. ESI-MS: *m/z* 485.23 ($M+H^+$).

*4.2.3.2. N-(3-((4-amino-3-(4-phenoxyphenyl)-1H-pyrazolo[3,4-d] pyrimidin-1-yl)methyl)phenyl) Acrylamide (**12b**)*. White solid, yield 52%, Mp: 173–174 °C, ^{1}H NMR (400 MHz, DMSO-d_6) δ 10.14 (s, 1H), 8.30 (s, 1H), 7.67 (d, J = 7.6 Hz, 4H), 7.52 (s, 1H), 7.43 (t, J = 7.4 Hz, 2H), 7.29 (t, J = 7.7 Hz, 1H), 7.24–7.08 (m, 6H), 7.03 (d, J = 7.3 Hz, 1H), 6.39 (dd, J = 16.9, 10.1 Hz, 1H), 6.23 (d, J = 16.8 Hz, 1H), 5.73 (d, J = 10.1 Hz, 1H), 5.53 (s, 2H). ^{13}C NMR (100 MHz, DMSO-d_6) δ 163.60, 158.69, 157.61, 156.76, 156.51, 154.85, 144.10, 139.73, 138.28, 132.24, 130.61, 129.52, 128.30, 127.45, 124.27, 123.34, 119.46, 119.00, 118.75, 97.72, 50.24. ESI-MS: *m/z* 463.04 ($M+H^+$).

4.3. In vitro BTK kinase inhibitory activity assay and kinase selectivity assay

The in vitro BTK kinase inhibitory activity and kinase selectivity were evaluated via a radiometric protein kinase assay. All compounds were prepared to 50 X final assay concentration in 100% DMSO. A portion of this working stock of the compounds was added to the assay well as the first component in the reaction, followed by adding kinases dilution with specific buffer. The reaction was initiated by the addition of the Mg/ATP mix. After incubation for 40 min at room temperature, the reaction was stopped by the addition of phosphoric acid to a concentration of 0.5%. 10 μL of the reaction was then spotted onto a P30 filtermat and washed four times for 4 min in 0.425% phosphoric acid and once in methanol prior to drying and scintillation counting. The inhibition rate was calculated by the following formula.

$$\text{Inhibition rate } \% = 1 - \frac{\text{Count}_C - \text{Count}_B}{\text{Count}_P - \text{Count}_B} * 100\%$$

Count_C: the counts of testing compounds.
Count_P: the counts of positive control. The positive control wells contained all components of the reaction, except the compound of interest, and DMSO (at a final concentration of 2%) was included in these wells to control for solvent effects.
Count_B: the counts of blank. The blank wells contained all components of the reaction with staurosporine, a reference inhibitor, replacing the compound of interest. This abolished kinase activity and established the baseline (0% kinase activity remaining).

IC_{50} values were calculated using the Graphpad prism 6 software.

4.4. Patient samples

Peripheral blood was obtained from MCL patients who provided informed consent. Mononuclear cells were separated by Ficoll-Hypaque density centrifugation, and tumor cells were isolated using anti-CD19 antibody coated magnetic microbeads (Miltenyi Biotec) and maintained in RPMI1640 medium (Life Technologies) supplemented with 10% heat-inactivated FBS, penicillin (10,000 U/mL, Sigma), streptomycin (10 mg/mL, Sigma).

4.5. Cell viability assay

MCL cell lines Mino, Jeko-1, Z138 and Maver-1 were purchased from the American Type Culture Collection ATCC). BTK knock out Jeko-1 cells were from the University of Texas MD Anderson Cancer Center. Primary MCL patient cells were purified from the apheresis of MCL patients after obtaining informed consent and approval by the Institutional Review Board at The University of Texas MD Anderson Cancer Center. Cells were cultured in RPMI-1640, supplemented with 10% heat-inactivated fetal bovine serum, 2% HEPES buffer and penicillin (10,000 units/mL; Sigma), streptomycin (10 mg/mL; Sigma). Cell viability assay was performed on MCL cell lines and primary MCL patient cells with the CellTiter-Glo Luminescent cell viability assay kit (Promega) following the manufacturer's protocol. In short, 50 uL cells were plated in 96-well plates at a density of 1×10^4 cells/well for MCL cell lines and 12.5×10^4 cells/well for primary MCL patient cells, then treated with DMSO (control) and different concentrations of the synthesized compounds in triplicate and incubated in a humidified atmosphere with 5% CO_2 at 37 °C for 72 h on MCL cell lines and 24 h on primary MCL patient cells. Cells were lysed with 30 uL Cell Titer-Glo Luminescent Cell Viability Assay Reagent (Promega, Madison, WI, USA), and luminescence was quantified using the BioTek Synergy HTX Multi-mode Micro Plate Reader (Winooski, VT, USA). Each triplicate experiment was performed no less than three times to establish the cell survival curve. IC_{50} values were calculated using the Graphpad prism 6 software.

4.6. Cell apoptosis assay

Apoptosis was quantified by Annexin V/Propidium Iodide (PI)-binding assay. Cells were seeded in 6-well plates with 1 μM and 2 μM of **12a** for 24 h. Treated cells were washed twice with cold phosphate-buffered saline (PBS) and then resuspended in 100 mL binding buffer, to which 2 mL of Annexin V-FITC and 5 mL of PI were added. The samples were gently vortexed and incubated for 15 min at room temperature in the dark. After addition of 200 mL binding buffer, samples were immediately analyzed by flow cytometry using a FACScan flow cytometer (Becton Dickinson, San Jose, CA). The number of apoptotic cells was determined using the Flowjo software.

4.7. Molecular docking

Molecular docking was performed using the Sybyl 2.0 software and the BTK crystal structure (PDB: 3gen) was retrieved from the Protein Data Bank. Protein preparation was performed by extracting the ligand, removing water molecules, adding hydrogen atoms and assigning AMBER7 FF99 charges to the protein. Compound **12a** was docked into BTK and the hydrogen bonds and hydrophobic interactions were observed in the model, the best conformation with the highest CScore was selected for interaction analysis.

4.8. Statistical analysis

Student's tests were performed for statistical analyses of **12a** induced apoptotic effect, two-way ANOVA analysis of variance was used to compare the **IBN** and **12a** treatment in the primary patient cells in *vitro*. P values of < 0.05 were considered statistically significant.

Acknowledgements

This work was supported by the key research and development project of Shandong Province [No. 2017CXGC1401].

References

[1] J.M. Vose, Mantle cell lymphoma: 2012 update on diagnosis, risk-stratification, and clinical management, Am. J. Hematol. 87 (2012) 604–609, https://doi.org/10.1002/ajh.23176.
[2] S. Nakamura, Y. Yatabe, M. Seto, Cyclin D1 overexpression in malignant lymphomas, Pathol. Int. 47 (1997) 421–429, https://doi.org/10.1111/j.1440-1827.1997.tb04519.x.
[3] P. Perez-Galan, M. Dreyling, A. Wiestner, Mantle cell lymphoma: biology, pathogenesis, and the molecular basis of treatment in the genomic era, Blood 117 (2011) 26–38, https://doi.org/10.1182/blood-2010-04-189977.
[4] Y. Liu, Y.Z. Yin, Z. Zhang, C.J. Li, H. Zhang, D.G. Zhang, C.Y. Jiang, K. Nomie, L. Zhang, M.L. Wang, G.S. Zhao, Structural optimization elaborates novel potent Akt inhibitors with promising anticancer activity, Eur. J. Med. Chem. 138 (2017) 543–551, https://doi.org/10.1016/j.ejmech.2017.06.067.
[5] P. Jares, D. Colomer, E. Campo, Genetic and molecular pathogenesis of mantle cell lymphoma: perspectives for new targeted therapeutics, Nat. Rev. Cancer 7 (2007) 750–762, https://doi.org/10.1038/nrc2230.
[6] R.W. Hendriks, S. Yuvaraj, L.P. Kil, Targeting Bruton's tyrosine kinase in B cell malignancies, Nat. Rev. Cancer 14 (2014) 219–232, https://doi.org/10.1038/nrc3702.
[7] S. Tsukada, D.C. Saffran, D.J. Rawlings, O. Parolini, R.C. Allen, I. Klisak, R.S. Sparkes, H. Kubagawa, T. Mohandas, S. Quan, J.W. Belmont, M.D. Cooper, M.E. Conley, O.N. Witte, Deficient Expression of a B-Cell Cytoplasmic Tyrosine Kinase in Human X-Linked Agammaglobulinemia, Cell 72 (1993) 279–290, https://doi.org/10.1016/0092-8674(93)90667-F.
[8] C.M. Lewis, C. Broussard, M.J. Czar, P.L. Schwartzberg, Tec kinases: modulators of lymphocyte signaling and development, Curr. Opin. Immunol. 13 (2001) 317–325, https://doi.org/10.1016/S0952-7915(00)00221-1.
[9] R. Kuppers, Mechanisms of B-cell lymphoma pathogenesis, Nat. Rev. Cancer 5 (2005) 251–262, https://doi.org/10.1038/nrc1589.
[10] Y. Aoki, K.J. Isselbacher, S. Pillai, Bruton tyrosine kinase is tyrosine-phosphorylated and activated in Pre-B lymphocytes and receptor-ligated B-cells, Proc. Natl. Acad. Sci. USA 91 (1994) 10606–10609, https://doi.org/10.1073/pnas.91.22.10606.
[11] T. Kurosaki, S. Tsukada, BLNK: Connecting Syk and Btk to calcium signals, Immunity 12 (2000) 1–5, https://doi.org/10.1016/S1074-7613(00)80153-3.
[12] P.L. Schwartzberg, L.D. Finkelstein, J.A. Readinger, TEC-family kinases: Regulators of T-helper-cell differentiation, Nat. Rev. Immunol. 5 (2005) 284–295, https://doi.org/10.1121/1.421093.
[13] Z. Zhang, D.G. Zhang, Y. Liu, D.Z. Yang, F.S. Ran, M.L. Wang, G.S. Zhao, Targeting Bruton's tyrosine kinase for the treatment of B cell associated malignancies and autoimmune diseases: Preclinical and clinical developments of small molecule inhibitors, Arch. Pharm. 351 (2018) e1700369, , https://doi.org/10.1002/ardp.201700369.
[14] O.J. D'Cruz, F.M. Uckun, Novel Bruton's tyrosine kinase inhibitors currently in development, Oncotargets Ther. 6 (2013) 161–176, https://doi.org/10.2147/OTT.S33732.
[15] R.C. Rickert, New insights into pre-BCR and BCR signalling with relevance to B cell malignancies, Nat. Rev. Immunol. 13 (2013) 578–591, https://doi.org/10.1038/nri3487.
[16] M.L. Wang, S. Rule, P. Martin, A. Goy, R. Auer, B.S. Kahl, W. Jurczak, R.H. Advani, J.E. Romaguera, M.E. Williams, J.C. Barrientos, E. Chmielowska, J. Radford, S. Stilgenbauer, M. Dreyling, W.W. Jedrzejczak, P. Johnson, S.E. Spurgeon, L. Li, L. Zhang, K. Newberry, Z.S. Ou, N. Cheng, B.L. Fang, J. McGreivy, F. Clow, J.J. Buggy, B.Y. Chang, D.M. Beaupre, L.A. Kunkel, K.A. Blum, Targeting BTK with Ibrutinib in Relapsed or Refractory Mantle-Cell Lymphoma, New Engl. J. Med. 369 (2013) 507–516, https://doi.org/10.1056/NEJMoa1306220.
[17] R.E. Davis, V.N. Ngo, G. Lenz, P. Tolar, R.M. Young, P.B. Romesser, H. Kohlhammer, L. Lamy, H. Zhao, Y.D. Yang, W.H. Xu, A.L. Shaffer, G. Wright, W.M. Xiao, J. Powell, J.K. Jiang, C.J. Thomas, A. Rosenwald, G. Ott, H.K. Muller-Hermelink, R.D. Gascoyne, J.M. Connors, N.A. Johnson, L.M. Rimsza, E. Campo, E.S. Jaffe, W.H. Wilson, J. Delabie, E.B. Smeland, R.I. Fisher, R.M. Braziel, R.R. Tubbs, J.R. Cook, D.D. Weisenburger, W.C. Chan, S.K. Pierce, L.M. Staudt, Chronic active B-cell-receptor signalling in diffuse large B-cell lymphoma, Nature 463 (2010) 88–92, https://doi.org/10.1038/nature08638.
[18] M. Cinar, F. Hamedani, Z.C. Mo, B. Cinar, H.M. Amin, S. Alkan, Bruton tyrosine kinase is commonly overexpressed in mantle cell lymphoma and its attenuation by Ibrutinib induces apoptosis, Leukemia Res. 37 (2013) 1271–1277, https://doi.org/10.1016/j.leukres.2013.07.028.
[19] B.Y. Chang, M. Francesco, M.F.M. De Rooij, P. Magadala, S.M. Steggerda, M.M. Huang, A. Kuil, S.E.M. Herman, S. Chang, S.T. Pals, W. Wilson, A. Wiestner, M. Spaargaren, J.J. Buggy, L. Elias, Egress of CD19(+)CD5(+) cells into peripheral blood following treatment with the Bruton tyrosine kinase inhibitor ibrutinib in mantle cell lymphoma patients, Blood 122 (2013) 2412–2424, https://doi.org/10.1182/blood-2013-02-482125.
[20] A. Akinleye, Y.M. Chen, N. Mukhi, Y.P. Song, D.L. Liu, Ibrutinib and novel BTK inhibitors in clinical development, J. Hematol. Oncol. 6 (59) (2013), https://doi.org/10.1186/1756-8722-6-59.
[21] J. Singh, R.C. Petter, T.A. Baillie, A. Whitty, The resurgence of covalent drugs, Nat. Rev. Drug. Discov. 10 (2011) 307–317, https://doi.org/10.1038/nrd3410.
[22] A. Aw, J.R. Brown, Current status of Bruton's tyrosine kinase inhibitor development and use in B-cell malignancies, Drugs Aging. 34 (2017) 509–527, https://doi.org/10.1007/s40266-017-0468-4.
[23] Z.Y. Pan, H. Scheerens, S.J. Li, B.E. Schultz, P.A. Sprengeler, L.C. Burrill, R.V. Mendonca, M.D. Sweeney, K.C.K. Scott, P.G. Grothaus, D.A. Jeffery, J.M. Spoerke, L.A. Honigberg, P.R. Young, S.A. Dalrymple, J.T. Palmer, Discovery of selective irreversible inhibitors for Bruton's tyrosine kinase, Chemmedchem 2 (2007) 58–61, https://doi.org/10.1002/cmdc.200600221.
[24] A. Noy, S. De Vos, C. Thieblemont, P. Martin, C.R. Flowers, F. Morschhauser, G.P. Collins, S. Ma, M. Coleman, S. Peles, S. Smith, J.C. Barrientos, A. Smith, B. Munneke, I. Dimery, D.M. Beaupre, R. Chen, Targeting BTK with Ibrutinib in Relapsed/ Refractory Marginal Zone Lymphoma, Blood 129 (2017) 2224–2232, https://doi.org/10.1182/blood-2016-10-747345.
[25] J.H. Lv, J.D. Wu, F. He, Y. Qu, Q.Q. Zhang, C.G. Yu, Development of Bruton's tyrosine kinase Inhibitors for Rheumatoid Arthritis, Curr. Med. Chem. 25 (2018) 5847–5859, https://doi.org/10.2174/0929867325666180316121951.
[26] C. Liang, D. Tian, X. Ren, S. Ding, M. Jia, M. Xin, S. Thareja, The development of Bruton's tyrosine kinase (BTK) inhibitors from, 2012 to 2017: A mini-review, Eur. J. Med. Chem. 151 (2018) 315–326, https://doi.org/10.1016/j.ejmech.2018.03.062.
[27] H.S. Walter, S.A. Rule, M.J.S. Dyer, L. Karlin, C. Jones, B. Cazin, P. Quittet, N. Shah, C.V. Hutchinson, H. Honda, K. Duffy, J. Birkett, V. Jamieson, N. Courtenay-Luck, T. Yoshizawa, J. Sharpe, T. Ohno, S. Abe, A. Nishimura, G. Cartron, F. Morschhauser, C. Fegan, G. Salles, A phase 1 clinical trial of the selective BTK inhibitor ONO/GS-4059 in relapsed and refractory mature B-cell malignancies, Blood 127 (2016) 411–419.
[28] E.K. Evans, R. Tester, S. Aslanian, R. Karp, M. Sheets, M.T. Labenski, S.R. Witowski, H. Lounsbury, P. Chaturvedi, H. Mazdiyasni, Z. Zhu, M. Nacht, M.I. Freed, R.C. Petter, A. Dubrovskiy, J. Singh, W.F. Westlin, Inhibition of Btk with CC-292 Provides Early Pharmacodynamic Assessment of Activity in Mice and Humans, J. Pharmacol. Exp. Ther. 346 (2013) 219–228, https://doi.org/10.1124/jpet.113.203489.
[29] J.K. Park, J.Y. Byun, J.A. Park, Y.Y. Kim, Y.J. Lee, J.I. Oh, S.Y. Jang, Y.H. Kim, Y.W. Song, J. Son, K.H. Suh, Y.M. Lee, E.B. Lee, HM71224, a novel Bruton's tyrosine kinase inhibitor, suppresses B cell and monocyte activation and ameliorates arthritis in a mouse model: a potential drug for rheumatoid arthritis, Arthritis Res. Ther. 18 (2016) 91, https://doi.org/10.1186/s13075-016-0988-z.
[30] N. Ding, X.T. Li, Y.F. Shi, L.Y. Ping, L.N. Wu, K. Fu, L.X. Feng, X.H. Zheng, Y.Q. Song, Z.Y. Pan, J. Zhu, Irreversible dual inhibitory mode: the novel Btk inhibitor PLS-123 demonstrates promising anti-tumor activity in human B-cell lymphoma, Oncotarget 6 (2015) 15122–15136, https://doi.org/10.18632/oncotarget.3824.
[31] J. Liu, D. Guiadeen, A. Krikorian, X. Gao, J. Wang, S.B. Boga, A.B. Alhassan, Y. Yu, H. Vaccaro, S. Liu, C. Yang, H. Wu, A. Cooper, J. de Man, A. Kaptein, K. Maloney, V. Hornak, Y.D. Gao, T.O. Fischmann, H. Raaijmakers, D. Vu-Pham, J. Presland,

M. Mansueto, Z. Xu, E. Leccese, J. Zhang-Hoover, I. Knemeyer, C.G. Garlisi, N. Bays, P. Stivers, P.E. Brandish, A. Hicks, R. Kim, J.A. Kozlowski, Discovery of 8-Amino-imidazo[1,5-a]pyrazines as Reversible BTK Inhibitors for the Treatment of Rheumatoid Arthritis, ACS Med. Chem. Lett. 7 (2016) 198–203, https://doi.org/10.1021/acsmedchemlett.5b00463.

[32] W. Kawahata, T. Asami, T. Irie, M. Sawa, Design and synthesis of novel pyrimidine analogs as highly selective, non-covalent BTK inhibitors, Bioorg. Med. Chem. Lett. 28 (2018) 145–151, https://doi.org/10.1016/j.bmcl.2017.11.037.

[33] W.B. Young, J. Barbosa, P. Blomgren, M.C. Bremer, J.J. Crawford, D. Dambach, C. Eigenbrot, S. Gallion, A.R. Johnson, J.E. Kropf, S.H. Lee, L. Liu, J.W. Lubach, J. Macaluso, P. Maciejewski, S.A. Mitchell, D.F. Ortwine, J. Di Paolo, K. Reif, H. Scheerens, A. Schmitt, X. Wang, H. Wong, J.M. Xiong, J. Xu, C. Yu, Z. Zhao, K.S. Currie, Discovery of highly potent and selective Bruton's tyrosine kinase inhibitors: Pyridazinone analogs with improved metabolic stability, Bioorg. Med. Chem. Lett. 26 (2016) 575–579, https://doi.org/10.1016/j.bmcl.2015.11.076.

[34] W.B. Young, J. Barbosa, P. Blomgren, M.C. Bremer, J.J. Crawford, D. Dambach, S. Gallion, S.G. Hymowitz, J.E. Kropf, S.H. Lee, L. Liu, J.W. Lubach, J. Macaluso, P. Maciejewski, B. Maurer, S.A. Mitchell, D.F. Ortwine, J. Di Paolo, K. Reif, H. Scheerens, A. Schmitt, C.G. Sowell, X. Wang, H. Wong, J.M. Xiong, J. Xu, Z. Zhao, K.S. Currie, Potent and selective Bruton's tyrosine kinase inhibitors: discovery of GDC-0834, Bioorg. Med. Chem. Lett. 25 (2015) 1333–1337, https://doi.org/10.1016/j.bmcl.2015.01.032.

[35] X.X. Li, A.L. Wang, K.L. Yu, Z.P. Qi, C. Chen, W.C. Wang, C. Hu, H. Wu, J.X. Wu, Z. Zhao, J. Liu, F.M. Zou, L. Wang, B.L. Wang, W. Wang, S.C. Zhang, J. Liu, Q.S. Liu, Discovery of (R)-1-(3-(4-Amino-3-(4-phenoxyphenyl)-1H-pyrazolo[3,4-d]pyrimidin-1-yl)piperidin-1-yl)-2-(dimethylamino)ethanone (CHMFL-FLT3-122) as a Potent and Orally Available FLT3 Kinase Inhibitor for FLT3-ITD Positive Acute Myeloid Leukemia, J. Med. Chem. 58 (2015) 9625–9638, https://doi.org/10.1021/acs.jmedchem.5b01611.

[36] B. Garcia-Reyes, L. Witt, B. Jansen, E. Karasu, T. Gehring, J. Leban, D. Henne-Bruns, C. Pichlo, E. Brunstein, U. Baumann, F. Wesseler, B. Rathmer, D. Schade, C. Peifer, U. Knippschild, Discovery of Inhibitor of Wnt Production 2 (IWP-2) and Related Compounds As Selective ATP-Competitive Inhibitors of Casein Kinase 1 (CK1) delta/epsilon, J. Med. Chem. 61 (2018) 4087–4102, https://doi.org/10.1021/acs.jmedchem.8b00095.